Article

JOURNAL OF COMPOSITE MATERIALS

Journal of Composite Materials
2023, Vol. 57(29) 4503–4519

DOI: 10.1177/00219983231211992
journals.sagepub.com/home/jcm
Sage

Extraction and characterization of novel natural cellulosic fiber from *Echinops spinosissimus* plant stem

Sid Ali Zernadji[1,2], Mansour Rokbi[1], Mohamed Benhamida[1] and Ahmed Kellai[3]

Abstract

Bio-based composites are outstanding materials to replace many synthetic fiber-based composites due to their biodegradability and sustainable environmental properties. This research aims to characterize and analysis a new cellulosic fibers extracted from *Echinops spinosissimus* plant stem, to study their integration in the field of various industries such as composites and textiles. Thus, adding and incorporating a new natural fiber to the list of fibers that enter into the production of Bio-based composites materials, and meet the needs of the market that knows a shortage of these materials. In addition, the extracted fibers from *Echinops spinosissimus* plant, which is abundant and have acceptable properties that can replace the synthetic fibers. The stem anatomy results showed a strong presence of fiber cells, fiber SEM micrographs showed that fiber surface become rough, these fibers have a density of 0.97 ± 0.01 g/cm^3, and diameter 280.76 μm. FTIR and XRD showed that these fibers are cellulosic. Thermal analysis revealed that *Echinops spinosissimus* fiber have a thermal stability of 208°C. Tensile strength, Young modulus and strain at failure were found as 217.54 ± 54.16 MPa, 19.23 ± 0.76 GPa and 3.78 ± 0.36%, respectively. SEM showed that the studied fiber becomes more roughness in the outer surface following the chemical treatments, thus contributing to better adhesion with resin. This work confirmed that *Echinops spinosissimus* fibers are suitable materials for use in textile and biocomposite applications.

Keywords

Echinops spinosissimus, stem anatomy, mechanical properties, attenuated total reflectance-fourier transform infrared spectroscopy, X-ray, thermogravimetric analysis

Introduction

Talking about natural fibers, research is still ongoing, especially in composites and textiles fields, thanks to its many and varied properties such as low density, non-toxicity, biodegradation, regeneration, low cost, thermal and mechanical properties.[1,2] These advantages have made natural fibers compounds among the most efficient materials with economic and environmental advantages. The quality of the fibers has an effective role in the performance of composite materials and are affected by the so-called extraction technique (chemical, mechanical, biological).[3]

Natural fiber composites are now considered a top-performing, cost-effective, and eco-friendly material category. The quality of the fibers used in these composites plays a significant role in determining the final product characteristics.[4] Researchers are continually assessing the mechanical properties, thermal stability, and durability of natural fiber composite materials. It is worth noting that the service life and performance of these materials may vary significantly depending on the used fiber type and composite formulation.[3]

The performance of plant fibers is directly affected by various factors such as maturity, growth environment (humidity, temperature, soil density),[3] and the method of extraction (chemical, mechanical, or biological). Additionally, the chemical treatment of natural fibers, such as alkali and potassium permanganate, can alter their properties, resulting in advantages like lower water absorption,

[1]Department of Mechanical Engineering, University of M'sila, M'sila, Algeria
[2]Laboratory of Materials and Mechanic of Structures (LMMS), University of M'sila, M'sila, Algeria
[3]Research Center in Industrial Technologies, Establishment, CRTI, Cheraga, Algeria

Corresponding author:
Mansour Rokbi, Department of Mechanical Engineering, University of M'sila, University pole of M'sila, M'sila, Algeria.
Email: mansour.rokbi@univ-msila.dz

increased surface roughness, higher thermal stability, and improved crystallinity index, less amorphous content, and increased crystallite size.[5]

As is known, natural fibers consist mainly of cellulose, hemicellulose, and some non-cellulose components (lignin, pectin and wax). Extraction techniques differ, but the goal is the same, which is to produce fibers with high mechanical properties by eliminating non-cellulosic components.[4] The choice of extraction technique is mainly related to the plant part where the fibers are found, as it may be found at the stem level (Inula viscosa, *Lygeum spartum*, *Atriplex halimus*),[6] Leaves (*Hyphaene thebaica*, Raffia textilis, *Furcraea foetida*),[2] Roots (*Cissus quadrangularis*, *Cyrtostachys renda*)[3] and fruits (Coconut, Cotton).[7]

These researchers characterize the lignocellulosic fibers as a reinforcement in composite materials, such as Banana.[8] Areca Catechu.[9] *Abelmoschus esculentus*.[10] Arundo *Donax*[11] and Grewia tilifolia.[12]

In recent years, due to the increasing demand and need for plant fibers, the amount of production did not cover the needs. This prompted researchers to strive to find and integrate new natural fibers, such as *Ficus religiosa*,[13] Date Palm,[14] Saharan aloe vera cactus.[15] *Vachellia farnesiana*.[16] Albizia Lebbeck[17] and *Juncus effusus*[18] for use in composites and textiles fields. Various plant species can be found in abundance in the region of M'sila – Algeria. The exploitation of new natural fibers from these plants, with acceptable mechanical and physical performances, can help increase the production of these materials, thus meet some demands around the world.

This study presents a new type of cellulosic fiber, which was extracted from the ES plant, called in Arabic "Chawki El Djabali", this type of plant spreads in abundance, especially in the hill and steppe regions in Msila Algeria. This investigation mainly aims to evaluate the possibility of using it as reinforcements in polymeric materials and textile industries.

This study showed that the *Echinops spinosissimus* fibers (ESFs) were extracted from the ES plant stems using an environmentally friendly biological method (immersion in fresh water).[19] To the best of our knowledge, this study is the first to explore, describe and characterize the *Echinops spinosissimus* fibers. Anatomy and surface morphologies were analyzed by using Binocular Motic Microscope (BMM) and Scanning Electron Microscopy (SEM). In the chemical analysis, the fibers samples were investigated with attenuated total reflectance-Fourier Transform Infrared spectroscopy (ATR-FTIR), X-ray diffraction (XRD) and the Energy-Dispersive X-Ray Spectroscopy (EDX). The thermal behavior was evaluated using thermogravimetric analysis (TGA). The mechanical behavior of this new cellulosic fiber was investigated using the single tensile tests procedure described in ASTM D-3322-01 Standard test method.[10]

Materials and methods

Plant materials

Echinops spinosissimus (ES) plant was harvested in May 2022 from Hodna region of Msila in Algeria (35°44'30"N, 4°32'30"E) as indicated in Figure 1. It is constituted of stems and can be recognized by its long cut leaves, with a clear central vein and lateral veins which end in a long white spine which grows to a height of 0.6 to 1 m. This plant belongs to the category of Asterales from Asteraceae family, genus: Echinops, Species: ES. The inflorescences form spheres 6 to 8 cm in diameter, bristling with long thorns (in fact bracts), hard, sharp and vulnerating which have earned them the English names "Thistle-ball". Between these thorns are formed the flowers composed of five white petals, welded in a tube at the bottom and nicely curved at the top.

Fibers extraction

The main purpose of extraction process is to produce stronger and undamaged fibers through the elimination of non-cellulosic components such as pectin, lignin and wax. In this paper, an environmentally friendly biological technique (microbial degradation) has been adopted. Figure 2 illustrate the main followed steps. For more details concerning this extraction. In the first time, leaves, dust and other foreign matter were removed from the stem of ES plant. After that, stems with diameter 8–15 mm were cut into lengths almost 50–70 cm. The obtained ES stems were washed with distilled water to remove the impurities and dirt more than one time to ensure their cleanliness. The principle of extraction consists of soaking ES stems, during 28 days (at room temperature), in a barrel filled with water and sodium bicarbonates (0.060%) to accelerate the bacterial decomposition.[7,20] After completion of retting period, every stem was crushed by a scraper so that only ES fibers remained.[2] The obtained ESFs were washed several times with distilled water to remove the deposits stuck on the surface, to leave them drip later for 24 h. Finally, the fibers have been dried in the oven at 70°C for 06 h with a view to getting rid of moisture.[17,21]

Chemical treatment

Two different chemical treatments were used in this investigation as shown in Table 1. The 3% alkaline and 0.033% permanganate, to improve the morphological and mechanical properties of ESFs.

Alkaline treatment. ESFs were immersed in distilled water with 3% sodium hydroxide solution (NaOH), for 3 h. The fibers were washed several times with distilled water by adding two drops of acetic acid (CH_3COOH) to reach a

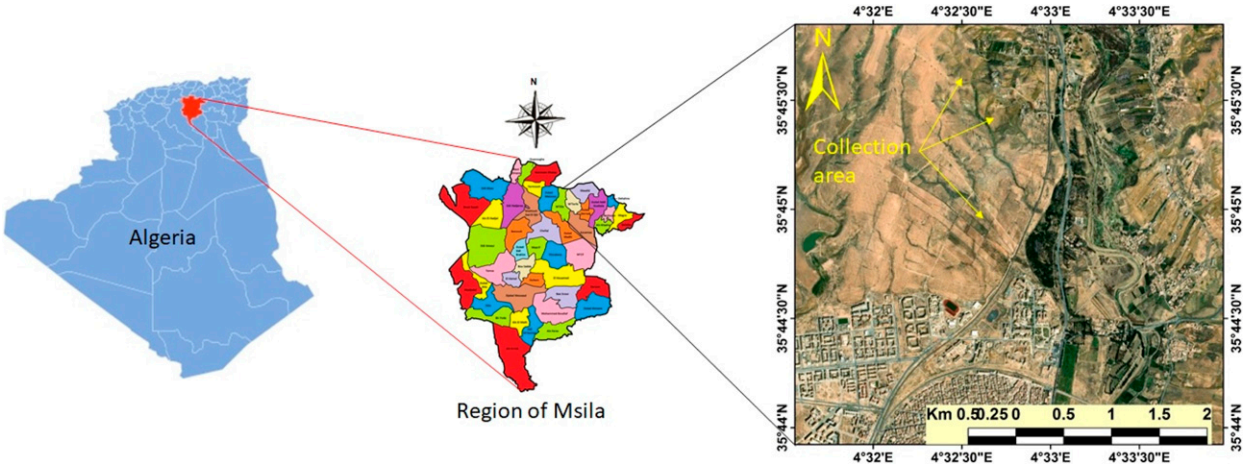

Figure 1. *Echinops spinosissimus* (ES) plant collection area.

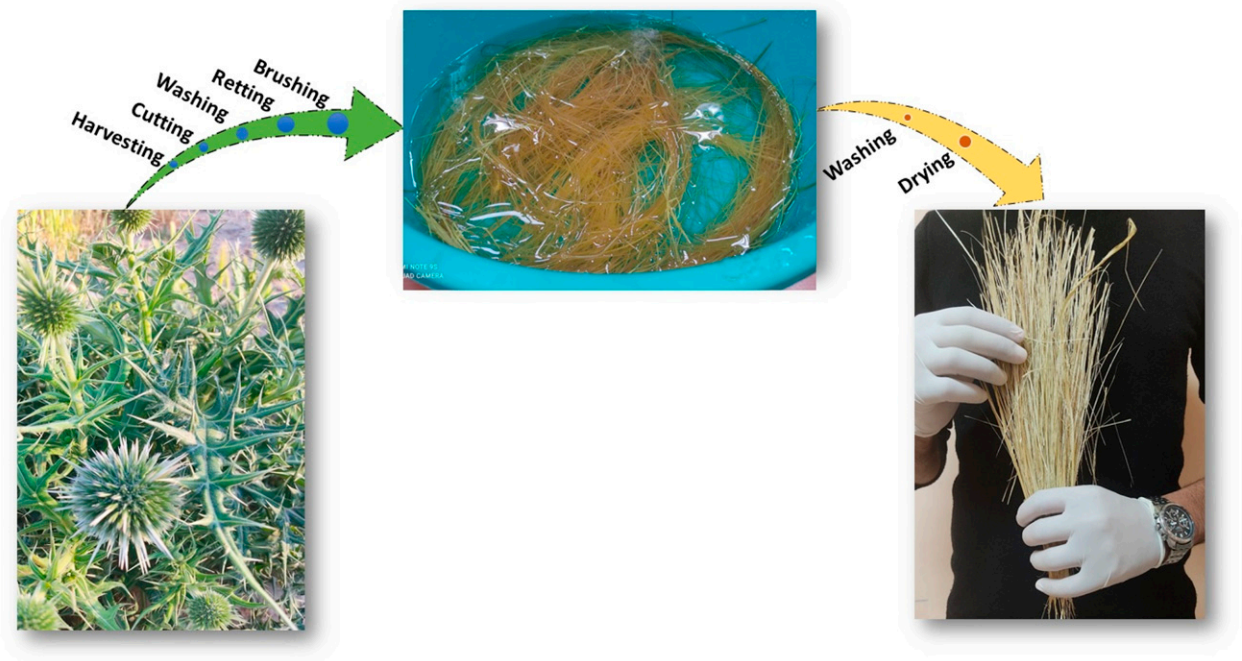

Figure 2. Extraction process of ESFs from the plant.

Table 1. Summary of chemical treatment techniques.

	Treatment		
Fiber	NaOH	$KMnO_4$	Designation
Raw Echinops spinosissimus fiber	/	/	R_{ESFs}
Alkali Echinops spinosissimus fiber	3%	/	A_{ESFs}
Permanganate Echinops spinosissimus fiber	3%	0.033%	P_{ESFs}

neutral pH. After rinsing and let it drip, the fibers were dried for 8 h before being characterized.

Permanganate treatment. For the permanganate treatment, ESFs pretreated with alkaline were soaked in 0.033% of Potassium permanganate ($KMnO_4$) solution for 3 min. These fibers were washed, neutralized and dried in the air for 48 h, before making various characterization.

Characterization methods

Echinops spinosissimus *stem anatomy*

By means of cutter, thin cross-sectional slices (0.3 – 0.8 mm) were taken from the stem of ES plant. Immersed in a methylene blue solution, and then cleaned with distilled water. Finally placed on a microscope slide with a coverslip to be examined using the OPTIKA optical microscope equipped with a camera connected to the computer to take pictures.

Physical properties

The density measurement for each one of the three types of ESFs was carried out by using a pycnometer for solids (50 mL), with immersion liquid known as the Ethanol ($\rho_{Eth} = 0.789$ g/cm^3). The measurements were carried out on a balance with 0.00001 g sensitivity. The analysis was performed at 28°C. Firstly, about 1 g of ESFs were cut into lengths of 1–5 mm. Then, they were dried at 80°C until their weight reached less than 95% of the initial weight in order to reduce the moisture content. Given ρ_{ESFs}, the density of ESFs (g/cm^3); ρ_{Eth}, the density of ethanol (g/cm$_3$); m^1, mass of empty pycnometer (g); m^2, mass of pycnometer with fibers (g); m^3, mass of the pycnometer filled with ethanol; m^4, mass of pycnometer with fibers and ethanol (g). The apparent density of ESFs is given by the formula (1):

$$\rho_{ESFs} = \left(\frac{m_2 - m_1}{(m_3 - m_1) - (m_4 - m_2)}\right)\rho_{Eth} \quad (1)$$

In order to obtain an average value for the diameter of each ESFs types, as supposed that the fiber has a cylindrical shape. A weighing process was carried out for more than 30 single fibers with a length of 200 mm for each one to get average ESFs mass using an analytical balance with a resolution of 0.00001 g. Then, the fiber cross section is calculated according to the following relationship (2):

$$S_f = \frac{M}{\rho_{ESFs} \times L} \quad (2)$$

where S_f, the fiber cross-section area; M, fiber mass; L, fiber length and ρ_{ESFs}, the fiber density. Finally, the diameters of ESFs are given by the formula (3):

$$D_{ESFs} = \sqrt{4M/(\rho_{ESFs} \times \pi \times L)} \quad (3)$$

Fourier transform infrared spectrometry (ATR-FTIR)

The FTIR analysis was carried out for three types ESFs by using an FTIR machine (Agilent Cary 630 FTIR Spectrometer, Malaysia) with spectral resolution of 2 cm^{-1}, and over wave number, range of 4000–500 cm^{-1} was used. The purpose of using ATR-FTIR analysis to distinguish the chemical composition and the changes in functional groups on the ESFs surfaces. The three types of ESFs were chopped and were ground into powder form in order to get the samples for this testing.

X-ray diffraction

The crystallinity degree of cellulosic ESFs were tested by using the XRD device (XRD, X'Pert Pro, EMPYREAN P Analytical, Netherlands) Physics laboratory at Msila university- Algeria. XRD testing is non-destructive and rapid testing. The tests were carried out for the raw fiber, 3% alkaline and 0.033% permanganate-treated ESFs. In this testing, by placing the ESFs samples on the sample holder in the form of a powder, the XRD device with a wavelength of 0.154 nm and a current of 30 mA and voltage of 40 kV. The continuous scanning mode, 2θ range varying from 10° to 60° with a speed of 4.67/min and step size of 0.02° at 28°C room temperature. The phase identification was accomplished by comparing the XRD signatures of the samples with the database provided by the Joint Committee on Powered Diffraction Standards (JCPDS). The crystallinity degree calculations of these samples of cellulosic ESFs were performed by the help of the data obtained from the XRD pattern. The crystallinity index (CI) of the three types ESFs was determined by Segal empirical technique displayed in equation (4):[5,22]

$$CI\% = \left[\frac{I_{002-I_{am}}}{I_{002}}\right] \times 100 \quad (4)$$

where, I_{200} represents the maximum intensity of the crystalline phase peak and I_{am} represents the amorphous phase's intensity in the cellulose present in the fiber.[23]

Thermogravimetric analysis

The thermal stability and thermal decomposition of raw, 3% alkaline and 0.033% permanganate-treated ESFs were obtained by Using TGA thermogravimetric analysis machine model (NETZSCH STA 409 PC/PG) Analytics Research Center Physico-Chemical "C.R.A.P.C" Laghouat - Algeria. after adjusting the temperature range between 20 and 700°C at a heating rate of 10°C/min under Nitrogen (N_2) atmosphere condition with a flow rate of (25 mL/min). A 30.613 mg sample mass of R_{ESFs}, 31.072 mg sample mass

of A_{ESFs} and 32.971 mg sample mass of P_{ESFs} were used for the test.

Fiber tensile testing

The tensile properties of ESFs were done according ASTM D3322-01 Standard, and were performed by using a Zwick/Roell tensile testing machine fitted with a 2.5 kN load cell. Tensile tests of single fibers was carried out for fiber length of 40 mm with crosshead speed of 2 mm/min. 30 specimens from each fibers type were prepared and tested to obtain the average values of tensile properties (Tensile strength, young's modulus and strain at failure). The tests are conducted at an ambient temperature 28°C with a relative humidity of about 68% ± 2% in accordance with ASTM D 3822 standard.

Scanning electron microscopy

The surface and ESFs morphology were examined using a thermo scientific Quattro Scanning Electron Microscopy FEG-SEM (USA), combines all round performance in imaging and analytics with a unique environmental mode (ESEM), to study samples in their natural state. The working distance was set between 3.1 and 13.4 mm, and the acceleration voltage of 2.0 kV. The images were taken by IR camera with two external signal inputs with image processor.

Energy-dispersive X-ray spectroscopy analysis

In terms of weight and atomic percentage, the Energy Dispersive X-ray Spectroscopy (EDX) was carried out to examine the element quantity in the ESFs specimens.

Results and discussion

Echinops spinosissimus *stem anatomy*

Figure 3 shows a cross-section view of fresh ES stem. Which consists of a relatively thin outer bark, below it are the fiber bundles, followed by vascular bundles. Distributed under the bark on a regular basis, but they differ in size and number, and this is due to several

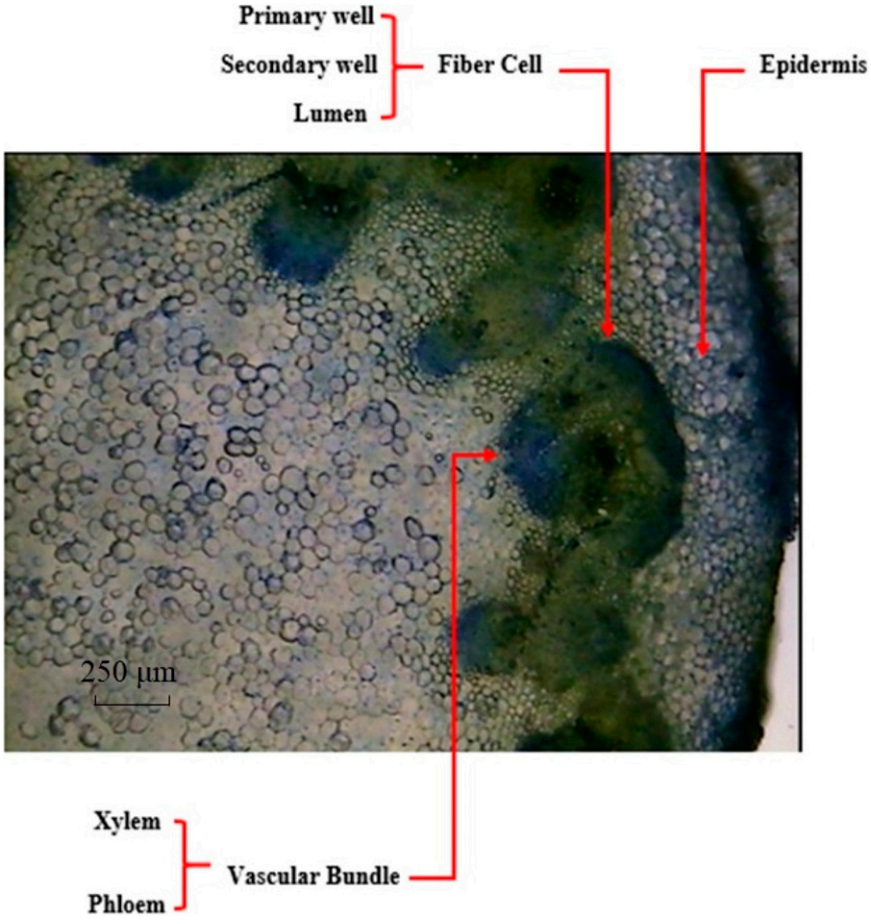

Figure 3. Microscopic image of ES stem transverse section.

internal and external factors, the most important of which is the age of the plant (maturity), the nature of soil and climate. This fiber bundles consist of a large number of fibers cells linked to each other by elements called lignin and hemicellulose together. We find that each fibers cell consists of a primary cell wall consisting of cellulose, followed by a secondary cell wall consisting of lignin, and in the middle, there are cells porosities or the so-called lumen, which help transport nutrients and other elements to various tissues with aqueous fluids. As for the vascular bundles, they consist mainly of xylem and phloem, exactly as mentioned in previous works report the anatomical investigations on natural fibers by several researchers such as *Centaurea melitensis*,[24] *Malva sylvestris* L.[25] and *Centaurea hyalolepis*.[26]

Physical properties

The density of natural cellulosic fibers is one of the criteria that focus on. Whenever the density of these fibers is lower, the composite materials reinforced with these fibers become lighter. This is what researchers seek to find, in contrast to the composite materials reinforced with synthetic fibers such as glass and carbon fibers, which are relatively heavy. In our research paper, using the ethanol pycnometer technique, the values of the densities of R_{ESFs}, A_{ESFs} and P_{ESFs} are 0.80 ± 0.06 g/cm^3, 0.93 ± 0.03 g/cm^3 and 0.97 ± 0.01 g/cm^3, respectively, those comparable with other fiber densities reported in previously article. Where an increase of ESFs density was observed. This is due to the fullness of pores and voids in the fibers surface, thanks to the chemical treatment. This values are situated in the (0.70 – 1.20 g/cm^3) range values of some natural cellulosic fibers densities (*Albizia lebbeck*, *Sansevieria cylindrica* and Rhectophyllum camerunense). The difference existing between the densities of natural cellulosic fibers is due to some parameters namely climatic conditions, nature of soil, maturity rate and extraction process. Thus, ESFs could be one of the candidate fibers for reinforcing lightweight materials.

As for speaking about diameters of R_{ESFs}, A_{ESFs} and P_{ESFs} were calculated as 336.52 µm, 305.34 µm and 280.76 µm, respectively. This is evidence of changes in ESFs diameters after chemical treatment of both types (Alkaline and Permanganate treatment), which led to the removal of lignin, pectin, wax and other impurities attached to the fibers surface. Where it was concluded that chemical treatment of cellulosic fibers improved their properties and developed its performance. This is consistent with the results of previous work.[27]

Fourier transform infrared spectrometry analysis (ATR-FTIR)

In this research section, several functional groups existing in ESFs with her three types are detected using FTIR analysis. FTIR spectra of R_{ESFs}, A_{ESFs} and P_{ESFs} are described in Figure 4. A large absorption band, observed around 3340 cm^{-1}, is attributed to the hydroxyl group (-OH).[4] Both peaks at 2921 cm^{-1} and 2862 cm^{-1} are associated to (CH2) groups of cellulose and hemicellulose.[11] The bands peaking at 1732 cm^{-1} correspond to hemicellulose carbonyl ester group C = O bond stretching. The wavenumber at 1592 cm^{-1} corresponds to the carbonyl groups (C = O) of lignin and hemicellulose,[28,29] while band at 1512 cm^{-1} indicates (C = C) groups of lignin.[16] The peak around 1457 cm^{-1} corresponds to the (CH_2) groups of cellulose. Then, the presence of peak around 1371 cm^{-1} is associated to (C-H) groups of cellulose.[30] The peak around 1325 cm^{-1} corresponds to the (C-H) groups of lignin.[6]The peak localized at 1237 cm^{-1} indicates (-COO) groups of hemicellulose. In addition, at 1158 cm^{-1} we found the (C-O-C) groups of cellulose and hemicellulose.[10,31] The wave number around 1024 cm^{-1} corresponds to the (C-O) groups of cellulose. Furthermore, the presence of a peak around 898 cm^{-1} is associated to (C-O) groups which are related to the β-glycosidic linkages.[16] Based on the above analysis, ATR-FTIR results have proved the existence of the main components (cellulose, hemicellulose, and lignin) in ESFs. Where the fibers FTIR spectra confirm the compositional changes in A_{ESFs} and P_{ESFs}. The peak at 1732 cm^{-1} was observed for R_{ESFs} spectrum, which correspond to hemicelluloses, disappeared for A_{ESFs} and P_{ESFs} spectrum. This result could be explained by the elimination of the residual hemicellulosic components after the Alkali and Permanganate treatments. In addition, much hemicellulose and others non-cellulosic components have been removed following NaOH and $KMnO_4$ treatment. This has been observed previously with sugar palm fiber.[32–34] The peak at 1237 cm^{-1} represents a significant decrease in the transmittance ratio of hemicelluloses. Finally, the peak at 1024 cm^{-1} represents an increment in the transmittance ratio of celluloses. It is to demonstrate that the increasing of celluloses and the removal of hemicelluloses and lignin from the two types of treated ESFs supports the results of the chemical analysis.[27,35] As a result, band positions differ between investigations.[30,36] Peak wave numbers in the FTIR spectrum and chemical composition stretch assignment of ESFs are summarized in Table 2.

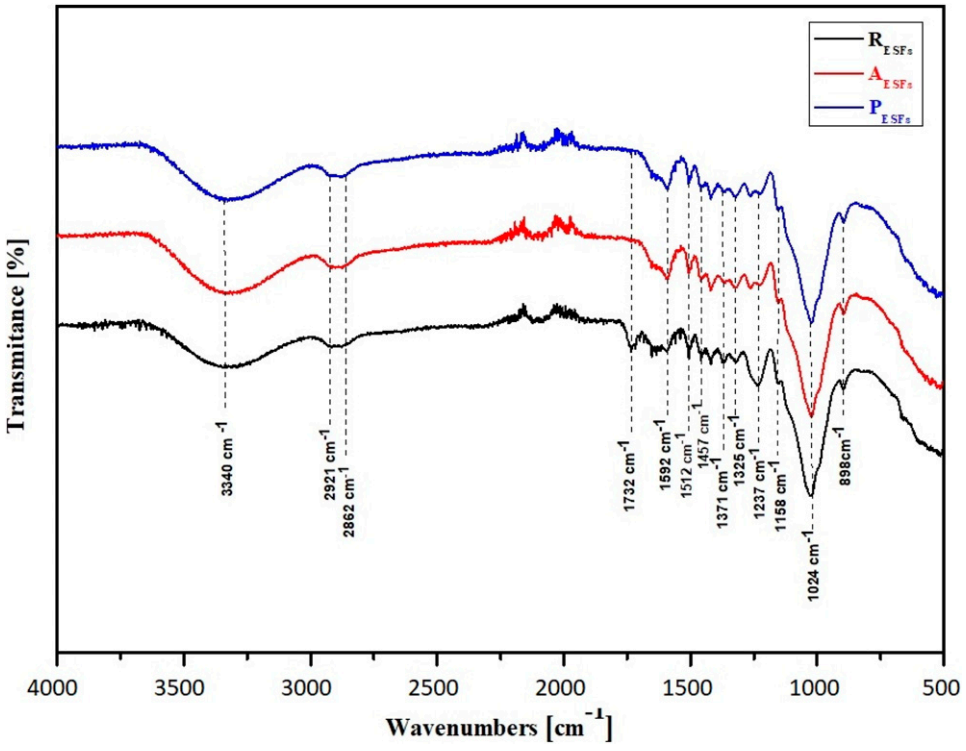

Figure 4. FTIR spectra of R_{ESFs}, A_{ESFs} and P_{ESFs}.

Table 2. Identification of peaks ATR-FTIR spectra of the ESFs.

Wave numbers (cm^{-1})	Vibrations mode(s)	Source(s)	References
3340	O–H stretching	Cellulose, hemicelluloses	1
2862–2921	C–H stretching	Cellulose, hemicelluloses	36
1732	C = O stretching	Hemicelluloses, lignin and extractives	29
1592	H–O–H bending of absorbed water	Water	36
1457–1512	H–C–H bending of absorbed water	Cellulose	33
1325–1371	C–H stretching	Lignin compounds	1
1237	-COO stretching	Hemicelluloses	34
1158	C–O bridge stretching	Cellulose	35
1024	C–O–C bridge stretching	Cellulose, hemicelluloses	31
898	β-glycosidic linkage	Cellulose, hemicelluloses	31

X-ray diffraction analysis

The XRD analysis revealed the crystallinity and structural characteristic of the ESFs before and after chemical treatments. Figure 5 illustrates the XRD pattern of the three types of ESFs and the corresponding planes involved. It was shown that each specimen showed two peaks and one amorphous plane I_{am}.[37] For R_{ESFs}, the first peak demonstrated at $2\theta = 16.55°$ represents the overlapped peak (110) which is peak of hemicellulose,[38] while for the second-high intensity peak demonstrated at $2\theta = 22.04°$ represents the main peak (200) of cellulose[1,38] which is crystalline peak. Then, as for A_{ESFs}, the first peak demonstrated at $2\theta = 16.32°$ represents the overlapped peak (110), while for the second-high intensity peak demonstrated at $2\theta = 22.19°$ represents the main peak (200) of cellulose which is crystalline peak. Finally, for P_{ESFs}, the first peak demonstrated at $2\theta = 16.84°$ represents the overlapped peak (110), while for the second-high intensity peak demonstrated at $2\theta = 22.17°$ represents the main peak (200) of cellulose which is crystalline peak. The I_{am} values of R_{ESFs}, A_{ESFs} and P_{ESFs} taken at the minimum in the

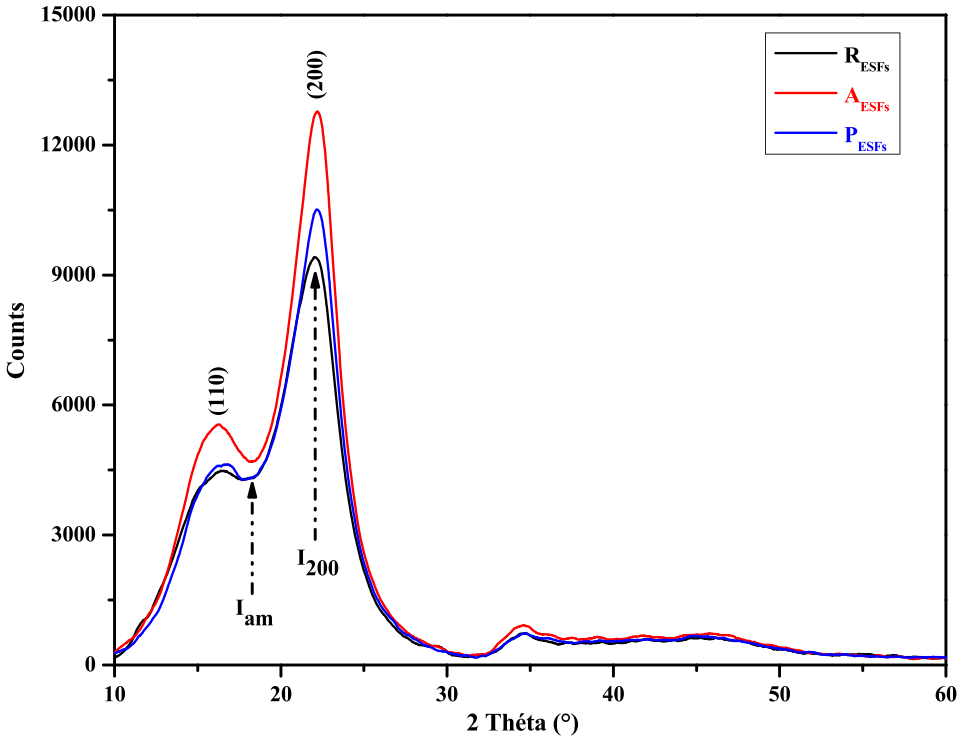

Figure 5. XRD pattern of R_{ESFs}, A_{ESFs} and P_{ESFs}.

intensity at about 17.67°, 18.11° and 17.69°, respectively.[39–41]

The value of crystallinity index (CI) was higher for A_{ESFs} at 63.28% followed by P_{ESFs} at 59.29% then R_{ESFs} at 54.64%. It was shown that fibers chemically treated with Alkaline and Permanganate were improved compared to raw fibers.[42–44] The higher index is attributed to removal of amorphous components and non-cellulosic materials,[1] improved hydrogen bond network, improved packing of cellulose chains, rearrangement of crystalline regions and loss of hydrophilic character.[5,45,46] This result agreed with SEM morphology, where the impurities of fiber were removed with chemical treatment.

The CI of ESFs with her three types is higher than that of *Juncus effusus* L, Grewia tilifolia, Pongamia Pinnata and Saharan *Aloe vera* cactus leaves, respectively 33.4%,[18] 41.70%,[12] 45.31%[47] and 52.6%.[15]

Thermogravimetric analysis

Figure 6(a), shows TG/DTG curves of R_{ESFs} with two weight loss steps are observed. The initial weight loss (6.07%) was observed between 29°C and 166°C, which represent the evaporation of water.[48–50] The second weight loss (89.97%) was seen between 190°C and 403°C with maximum decomposition rate at 310°C. This loss rate corresponds to the decomposition of cellulose I and α-cellulose.[11] After that, the weight loss was pursued until 700°C with a loss rate of about 97.60%. Figure 6(b) represents TG/DTG curves of A_{ESFs} show two weight loss steps. The initial weight loss (6.52%) was similar to the R_{ESFs} between 30°C and 173°C. And also represents the evaporation of water.[48] The second weight loss (81%) was observed between 203°C and 365°C with maximum decomposition rate at 295°C. This loss rate corresponds to the degradation of cellulosic components.[51] After that, the weight loss was pursued until 700°C with a loss rate of about 96.37%. Then, Figure 6(c) shows TG/DTG curves of P_{ESFs} with two weight loss steps are observed. The initial weight loss (4.72%) between 39°C and 183°C. And also represents the evaporation of water.[48,52] The second weight loss (81%) was observed between 208°C and 380°C with maximum decomposition rate at 287°C. This loss rate corresponds to the degradation of cellulosic components.[51] After that, the weight loss was pursued until 700°C with a loss rate of about 94.30%. According to the thermal analysis, it was shown that the maximum decomposition temperature of the chemically treated fibers were higher than the maximum decomposition temperature of the raw fibers. Onset degradation temperature of R_{ESFs}, A_{ESFs} and P_{ESFs} were obtained to be 190°C, 203°C and 208°C, respectively. It was clearly showed that chemical treatment led to increase the onset degradation temperature of fibers by decreasing the relative content of hemicellulose.[4,53,54]

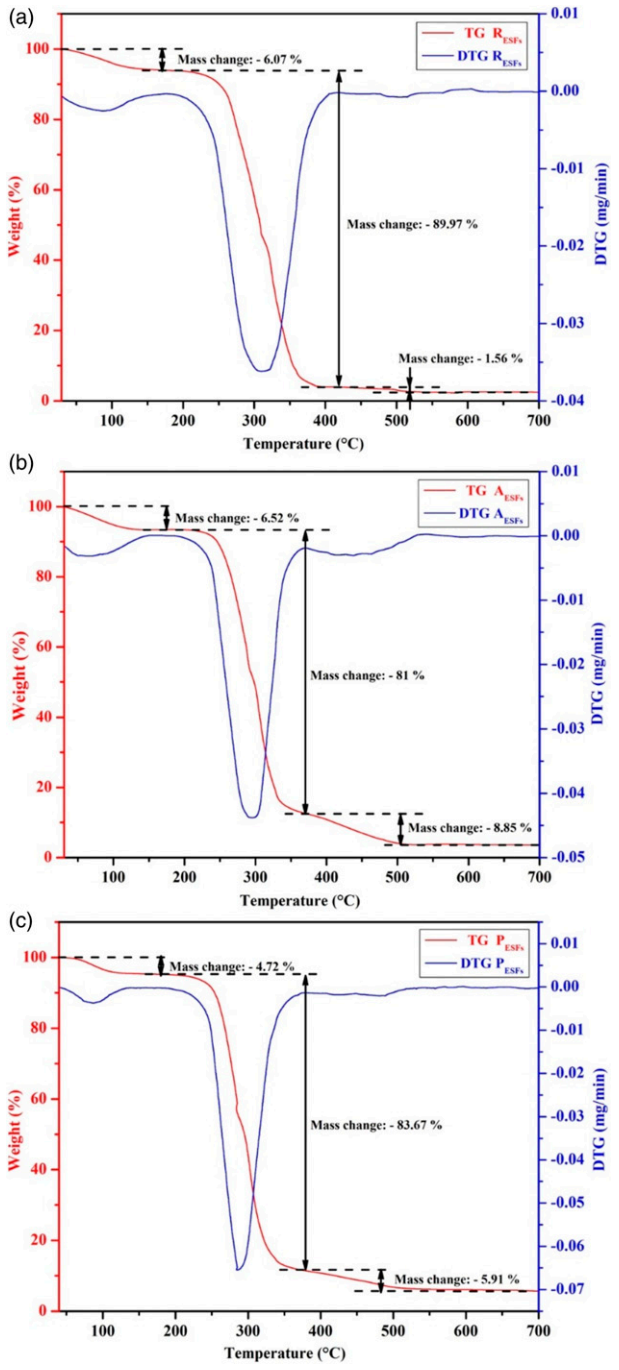

Figure 6. Thermogravimetric curves (TG and DTG) of: (a) R_{ESFs}, (b) A_{ESFs} and (c) P_{ESFs}.

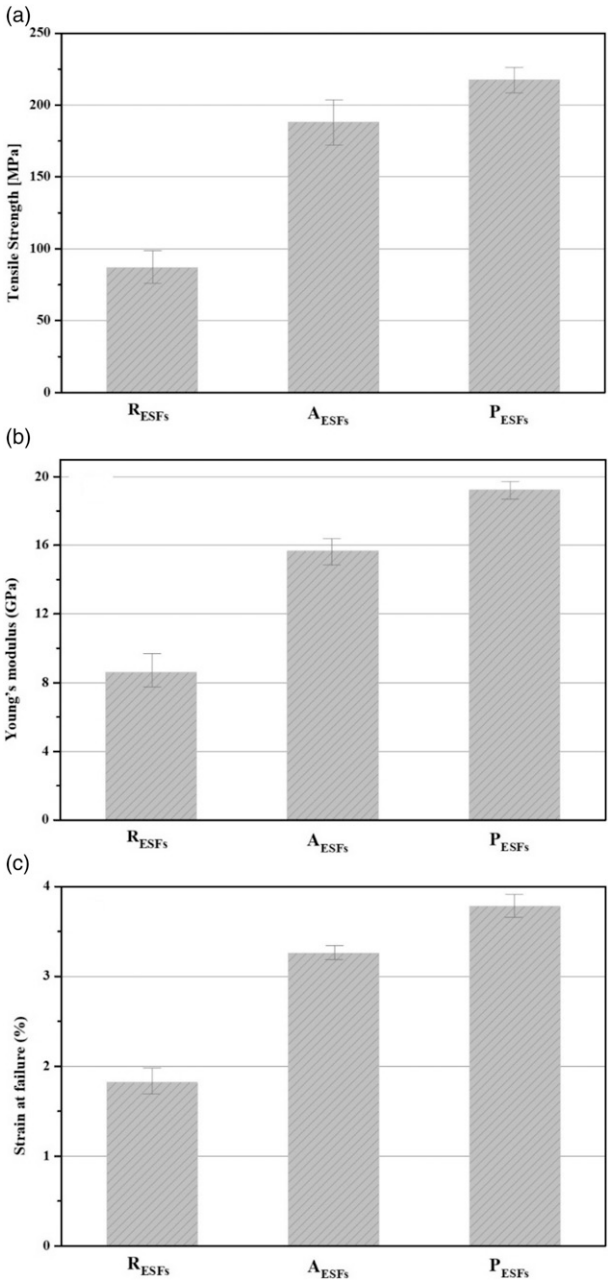

Figure 7. Mechanical properties of R_{ESFs}, A_{ESFs} and P_{ESFs}: (a) Tensile strength, (b) Young's modulus and (c) strain at failure.

Tensile test of the Echinops spinosissimus *fibers*

The mechanical properties study of natural fiber reinforced polymer composites or for textile is important to understand their potential for various structural applications and play a critical role in deciding the use of natural fibers. Figure 7(a) compares the tensile strength of the three types of ESFs specimens with length of 40 mm. As shown in this Figure, the tensile strength trend was increasing for A_{ESFs} and P_{ESFs} compared to R_{ESFs} for all tested samples with values of 188.16 ± 36.28 MPa, 217.54 ± 54.16 MPa and 87.09 ± 9.41 MPa, respectively. The increased tensile strength of chemically treated ESFs due to elimination of impurities from the ESFs surface and increasing ratio of cellulose.[55]

Table 3. Comparison for physical and mechanical properties of CDAFs with other cellulosic fibers.

Plant species	Density (g/cm^3)	Diameter (μm)	Tensile strength (MPa)	Young's modulus (GPa)	Strain at failure (%)	References
Stippa tenacissima	0.89–2.10	6–22	134–264	11–22	1.5–5.8	7
Hyphaene thebaica	1.36	165.81	215.98–593.35	12.79–24.29	1.51–2.92	2
Inula viscosa	78.60	1.154	196.99	12.98	1.57	6
Atriplex halimus	1.466	214–531	64.31–229.26	6.60–19.38	0.97–2.61	1
Lygeum spartum	—	180–433	64.63–280.03	4.47–13.27	1.49–3.74	4
Chrysanthemum m	1.336	—	65.12	1.55	4.51	49
Ficus religiosa tree	1.27	22.54	530.3	8.02	6.60	50
Arundo donax	1.168	—	60–80	3.6–4.0	2.5–3.5	11
Phaseolus vulgaris	0.96	345	523	10.64	1.63	54
Vakka	—	—	549	15.85	3.46	20
Date palm	—	—	170–275	5–12	5–10	14
Albizia lebbeck	0.90	—	270	67.45	2.57	17
Centaurea melitensis	1.269	187.11	336.87	23.87	1.27	24
Strelitzia reginae	1.075	170	269.45	12.30	3.43	36
Kigelia africana	1.31	0.50–0.62	50.31–73.12	2.17–39.84	0.15–2.98	52
Sansevieria cylindrica	0.915	—	673.12	6.72	10.04	55
Vachellia farnesiana	1.270	231	33.075	—	—	23
Thespesia lampas	—	—	573	61.2	0.79	28
Prosopis juliflor	0.58	20	558	—	1.77	48
Furcraea foetida	0.77	12.8	612.43	6.44	10.45	57
Banana	—	0.17–0.21	222.3	6.6	3.27	8
Raw ESFs	0.8	336.52	87.09	8.63	1.82	Current work
Alkaline ESFs	0.93	305.34	188.16	15.68	3.26	
Permanganate ESFs	0.97	280.76	217.54	19.23	3.78	

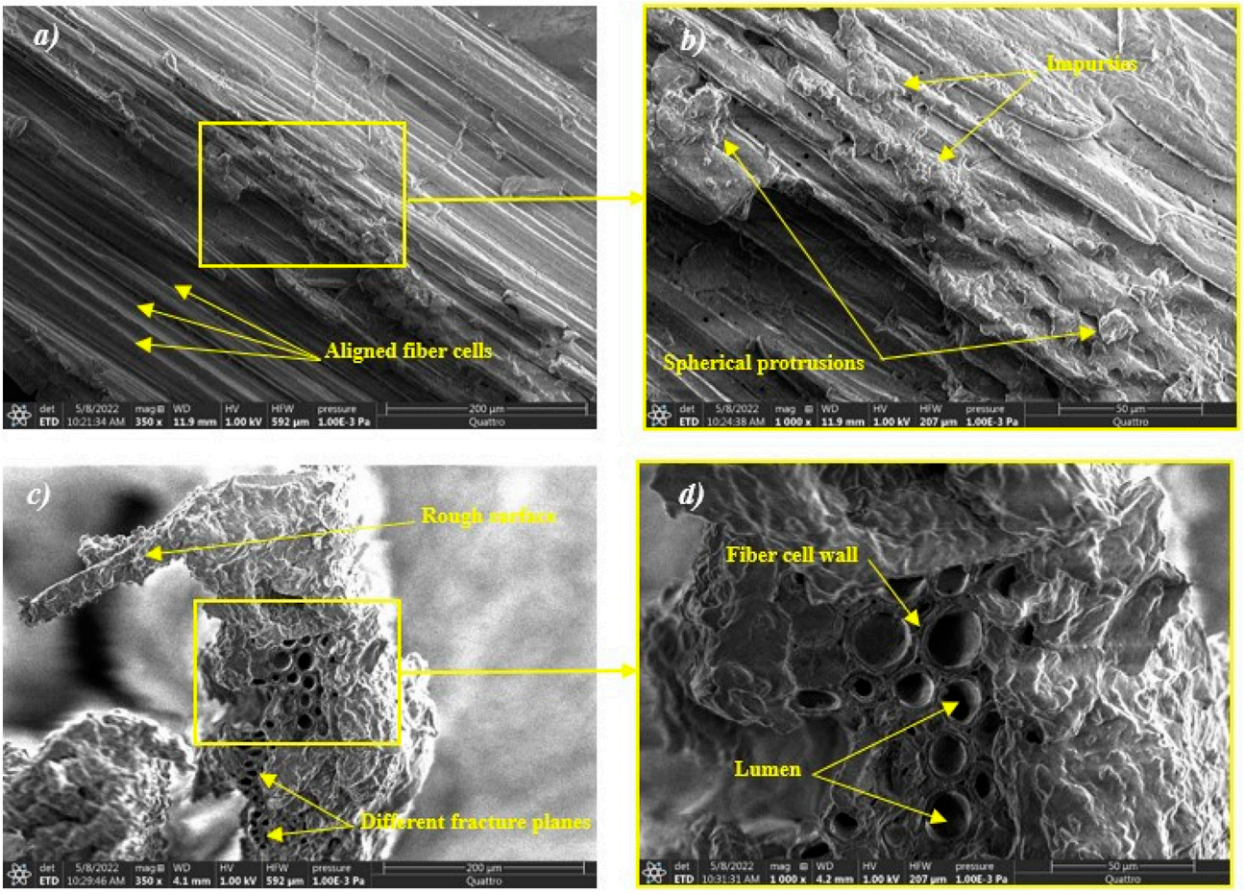

Figure 8. SEM micrographs of R_{ESFs}: (a) & (b) longitudinal section and (c) & (d) cross-section.

Previous research shows the values of tensile strength from plants fiber was approximate with ESFs such as Lygeum Spartum (64–280 MPa),[4] *Hyphaene thebaica* (215.98–593.35 MPa).[2] Note that ES tensile strength is less than Vakka (549 Mpa)[20] and Centaurea Melitensis (336.87 MPa),[24] and is higher than that of Stippa tenacissima (134–264 Mpa),[7] Inula viscosa (196.99 Mpa)[6] and *Kigelia africana* (50–73 Mpa).[52] Figure 7(b), represents the main values of Young modulus of R_{ESFs}, A_{ESFs} and P_{ESFs}, which were 8.63 ± 1.12 GPa, 15.68 ± 0.87 GPa and 19.23 ± 0.76 GPa, respectively. The tensile modulus of A_{ESFs} and P_{ESFs} were higher than of R_{ESFs} for all tested samples. The values were quite approaching to other plant fiber such as Banana (8–20 GPa)[8] and sisal (6.7–21.7 GPa).[56] The brittle nature of the material causes rapid collapse of the fibers due to the main components such as lignin, wax and hemicellulose.[24] However, after treating the ESF chemically (alkaline and permanganate treatment), the mechanical properties were improved significantly and the values of Young's modulus of elasticity increased. This is due to the fiber performance, which is mainly summed up by elimination of non-cellulosic components. Figure 7(c), shows the strain rate of three types of ESFs, the strain rate of R_{ESFs}, A_{ESFs} and P_{ESFs} were 1.82 ± 0.28%, 3.26 ± 0.17% and 3.78 ± 0.36%, respectively, directly affects the micro fibrillation angle of the ESFs. This finding agrees with the above discussion that Alkaline and Permanganate treatment increases the values of Young's modulus and tensile strength.[57,58] The mechanical tests results confirmed that ESFs could be used as reinforcement of polymers. A comparison of physical and mechanical properties of ESFs with recent similar works in this area are given in Table 3.

Scanning electron microscopy analysis

Scanning electron microscopy analysis of R_{ESFs}. Longitudinal and cross-sectional view of R_{ESFs} are shows in Figure 8(a–d). The longitudinal view of the fiber in Figure 8(a) shows a non-degraded fiber with a rather

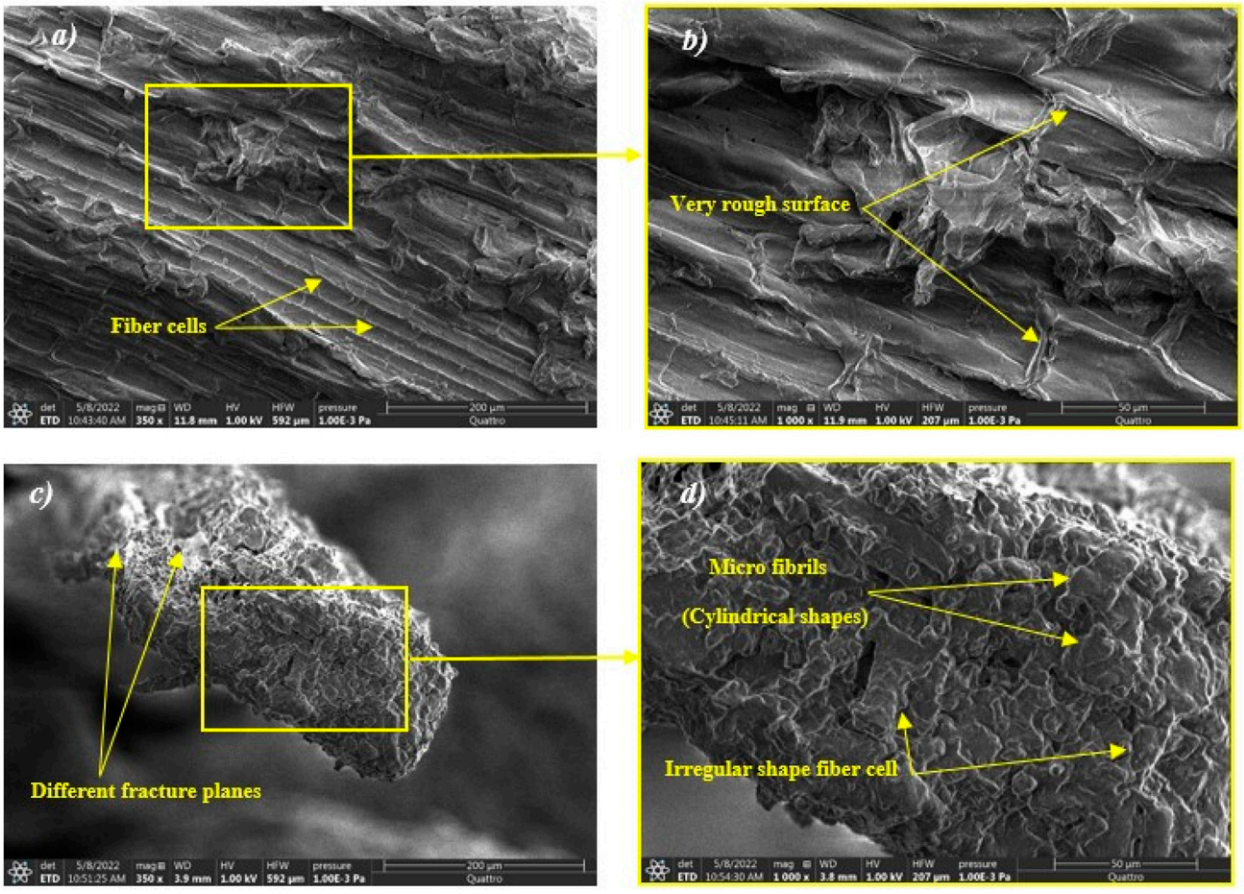

Figure 9. SEM micrographs of A_{ESFs}: (a) & (b) longitudinal section and (c) & (d) cross-section.

rough surface, where it can be clearly seen that the fiber bundles contain a large number of fiber cells with irregularity in diameter are aligned parallel to a single axis and bounded together by lignin, wax and hemicellulose. Further magnification in Figure 8(b), shows the presence of impurities and a number of spherical protrusions that provides good bonding with the polymer matrix[59] as mentioned in previous works on natural fibers such as Lygeum Spartum L.[4] and Vachellia farnesiana.[16] The cross-sectional view shown in Figure 8(c) reveals bundles of micro fibrils bounded together by non-cellulosic compounds. These micro fibrils have a rough surface like demonstrated in this Figure, where almost all fibrils have minimum angle deviation with fiber axis, which supports the angle of the microfibers, and cause a different fracture plane as shown in this Figure. Where Figure 8(d), represents a zoom magnification shows a group of porous cells and many cavities of different shapes and sizes (circular, triangular, irregular …). These cavities called lumen affect the diameter of the fibers cells, which directly affects the mechanical properties of the fibers.

Scanning electron microscopy analysis of A_{ESF}. The SEM micrographs in Figure 9(a)–(d), show the morphology of Alkali treated ESFs. Figure 9(a), shows a general longitudinal view of A_{ESFs} reveals a large number of fibers cells aligned and bounded together by lignin and hemicellulose. It can be clearly seen that surface of A_{ESFs} become very rough surface suitable for a good bond with polymer matrix compared to raw fiber.[59] Figure 9(b), is the zoom of Figure 9(a), It can be note that there is no presence of impurities such as wax and grease thanks to the treatment by 3% alkaline. Figure 9(c), represent a cross section micrograph of A_{ESFs} and show different fracture planes. Figure 9(d), is the zoom of Figure 9(c), where it can be clearly seen a change in the shapes of fiber bundles due to the filling up of the lumen (pores and voids) as a result of the treatment. Where chemical treatment by 3% alkaline affects the components ratios of these fiber cells parts (cellulose, hemicellulose and lignin). As previously mentioned in density measurement, (FTIR) and (XRD) analysis, the percentage of cellulose increased, and this is what is proven, these cylindrical shape of fiber cells positively affect the mechanical properties of ESFs to make it perform much

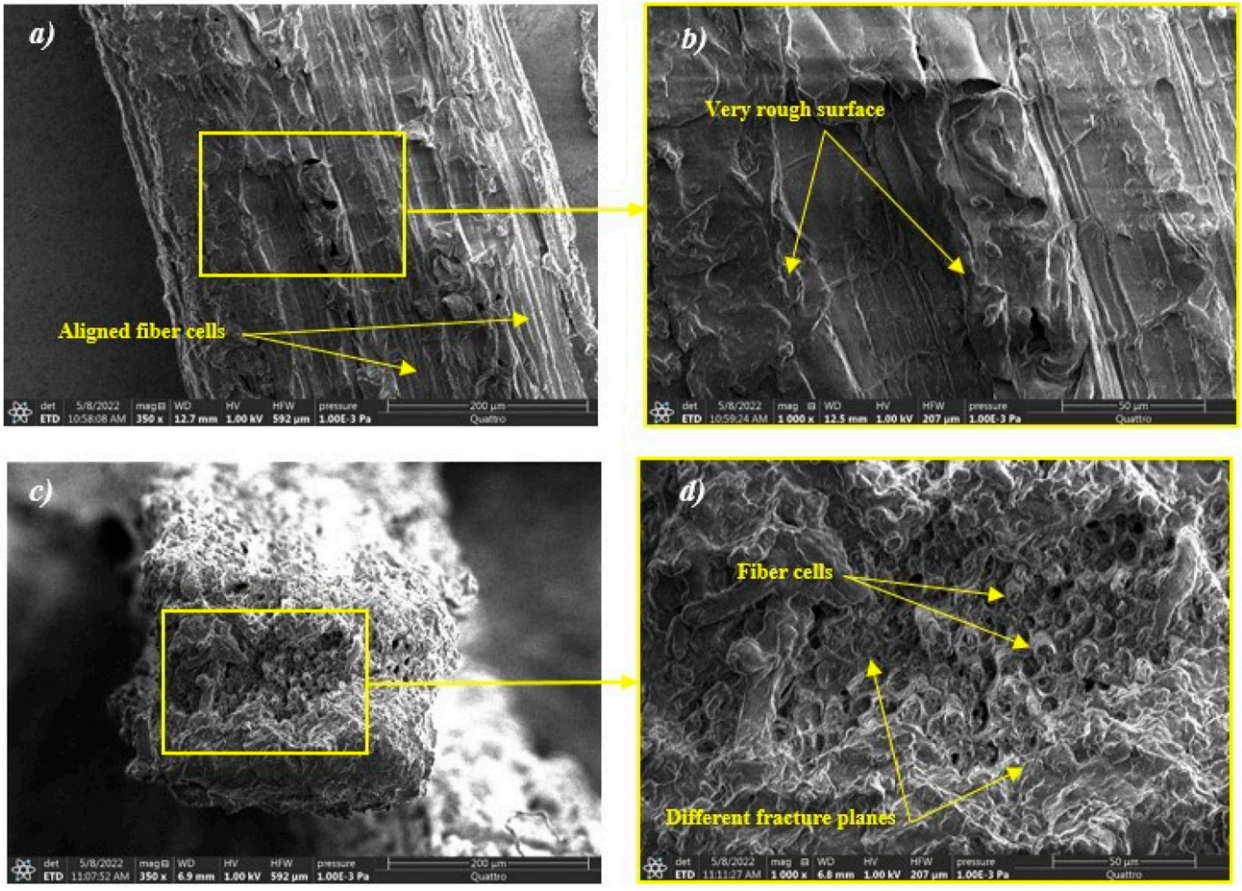

Figure 10. SEM micrographs of P_{ESFs}: (a) & (b) longitudinal section and (c) & (d) cross-section.

better by increasing Young's modulus and tensile strength. This result is consistent with previous discussions, same observations are reported in other works such as *Strelitzia reginae*.[36]

Scanning electron microscopy analysis analysis of P_{ESFs}. The SEM micrographs in Figure 10(a)–(d), illustrate the morphology of Permanganate treated ESFs. Figure 10(a), gives a general longitudinal view of P_{ESFs}, with aligned fiber cell. Figure 10(b), is the zoom of Figure 10(a), it can be clearly seen that these fibers have a very rough surface suitable for a good bond with matrix polymer compared to raw fiber.[59] It can also be noted that apparently, there is no presence of impurities such as wax and grease, this is basically due to both processes (pretreatment by 3% Alkaline and treatment by 0.033% Permanganate). Figure 10(c), represent a cross section micrograph of P_{ESFs}. Figure 10(d), is the zoom of Figure 10(c), where it can be clearly seen a change in the shapes of fiber bundles to become cylindrical, called microfibril due to the filling up of the lumen (pores and voids) on R_{ESFs} surfaces as a result of the treatment and show different fracture planes for almost of fiber cells. The chemical treatment by 0.033% Permanganate effect on the fiber components ratios (cellulose, hemicellulose and lignin) seem to be close to that of treatment by 3% alkaline. Where the percentage of cellulose increased, as previously proven in density measurement, and mentioned in (FTIR) and (XRD) analysis, these cylindrical shape of fiber cells positively affect the mechanical properties of the fibers to make it perform much better by increasing the tensile strength and Young's modulus. This result is in accordance with other reported works.[2]

Energy-dispersive X-ray spectroscopy analysis

Figure 11(a–c) reveal the presence of various elements and their distribution in the R_{ESFs}, A_{ESFs} and P_{ESFs}, respectively. The presence of Carbon (C), Oxygen (O), Calcium (Ca), Manganese (Mn), Arsenic (As), Neon (Ne), Sodium (Na), Magnesium (Mg) and Silicon (Si) is clearly observed in the distributions. In other words, studying the Energy-Dispersive X-Ray Spectroscopy can give a better understanding of the elements composition

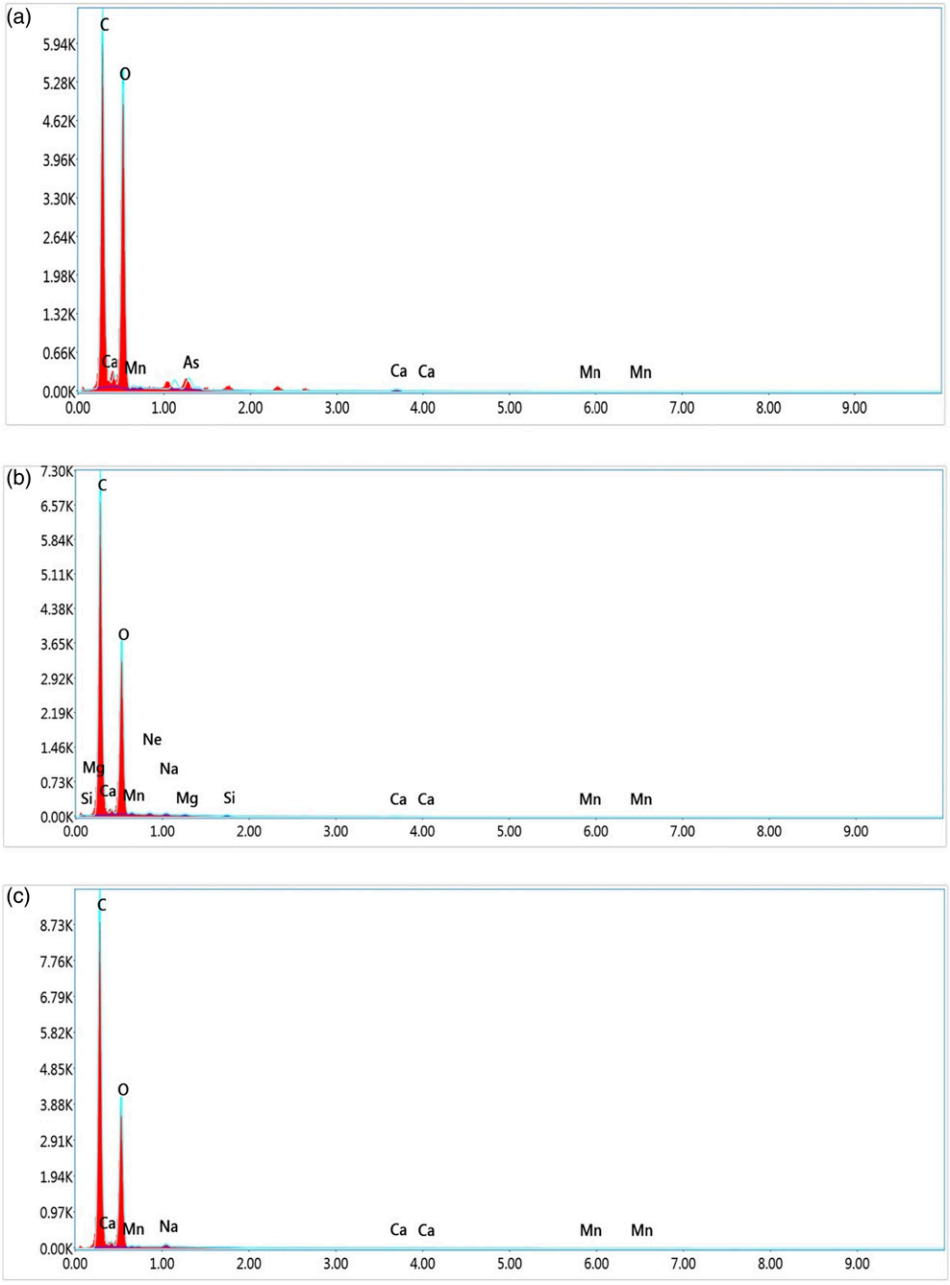

Figure 11. EDX analysis of: (a) R_{ESFs}, (b) A_{ESFs} and (c) P_{ESFs}.

Table 4. Weight and atomic percentages of each element of the three type of ESFs and various other fibers.

Fibers	R_{ESFs}		A_{ESFs}		P_{ESFs}		*Ficus religiosa* root[50]	
Elements	Weight (%)	Atomic (%)	Weight (%)	Atomic (%)	Weight (%)	Atomic (%)	Weight (%)	Atomic (%)
C	45.93	54.94	55.88	63.36	70.36	76.10	67.48	75.5
O	48.75	43.76	41.88	35.65	29.17	23.68	25.32	21.27
Ne	—	—	0.28	0.19	—		—	
Na	—	—	0.44	0.26	0.31	0.17	2.71	1.58
Mg	—	—	0.21	0.12	—	—	—	—
Si	—	—	0.24	0.12	—	—	—	—
Ca	1.35	0.48	0.49	0.17	0.16	0.05	—	—
Mn	0.81	0.21	0.58	0.14	0.00	0.00	—	—
As	3.16	0.61	—		—	—	—	—
Cl	—	—	—		—	—	3.11	1.18
K	—	—	—		—	—	1.37	0.47

of natural fibers for their subsequent use as a reinforcing element, especially in thermoplastic-matrix composites.

The weight and atomic percentages of each element of ESFs with her three types along with other fibers are shown in Table 4. The weight percentage of C and O is more than the other elements present in the EDX analysis, also the atomic percentage of C and O is more than the other elements in the EDX analysis, as usually seen in most cellulosic fibers such as *Ficus religiosa* root.[50]

Conclusion

This study presents the extraction process and characterization of new cellulosic fibers from ES plant stem to evaluate their potential use in textiles and as reinforcement in composite products. The morphological, physical, chemical, thermal and mechanical analysis were discussed in detail and the results were reported in this work were drawn:

- Stem anatomical structure showed that ES plant is rich in cellulosic fibers, fiber cells linked into bundles by middle lamellae, and so the vascular bundles are composed mainly of xylem and phloem tubes.
- FTIR analysis confirmed that ESFs contain cellulose and have water absorption capacity, as the percentage of cellulose increased after treatment and the fibers became hydrophobic.
- ESFs treated with Alkaline and Permanganate solution eliminated lignin and hemicellulose, increased the crystallinity index to reach value 59.29%–63.28% and the thermal stability, making the ESFs usable as the reinforcing component of a composite material processed at temperatures up to 208°C.
- EDX analysis showed that the most ESFs weight percentage components represents C and O which is cellulose.
- ESFs are characterized by low density (0.80– 0.97 g/cm^3) compared to synthetic ones, and relatively small diameters (280.76–336.52 µm) compared to other fibers, making it suitable as reinforcement for composite materials used in light-weight applications.
- Tensile strength reached 217.54 ± 54.16 MPa for single fiber obtained from treated ESFs with $KMnO_4$, the Young's modulus was 19.23 ± 0.76 GPa, while the strain at break of P_{ESFs} was 3.78 ± 0.36%.
- The SEM micrographs show that NaOH and $KMnO_4$ treatment yielded rough-surfaced fibers and filled lumen of fiber bundles to become cylindrical microfibril.

Through the obtained results, the ESFs possess many good characteristics qualify this new fiber as potential cellulosic fibers source, and as a good candidate for textile and composite applications.

Declaration of conflicting interests

The author(s) declared no potential conflicts of interest with respect to the research, authorship, and/or publication of this article.

Funding

The author(s) received no financial support for the research, authorship, and/or publication of this article.

ORCID iDs

Sid Ali Zernadji https://orcid.org/0000-0002-9303-7229
Mansour Rokbi https://orcid.org/0000-0001-5856-662X

References

1. Belouadah Z, Toubal LM, Belhaneche-Bensemra N, et al. Characterization of ligno-cellulosic fiber extracted from Atriplex halimus L. plant. *Int J Biol Macromol* 2021; 168: 806–815.
2. Mansour R, Abdelaziz A and Fatima Zohra A. Characterization of long lignocellulosic fibers extracted from Hyphaene thebaica L. leaves. *Research Journal of Textile and Apparel* 2018; 22: 195–211.
3. Loganathan TM, Hameed Sultan MT, Ahsan Q, et al. Characterization of alkali treated new cellulosic fibre from cyrtostachys renda. *J Mater Res Technol* 2020; 9: 3537–3546.
4. Belouadah Z, Ati A and Rokbi M. Characterization of new natural cellulosic fiber from Lygeum spartum L. *Carbohydr Polym* 2015; 134: 429–437.
5. French AD and Santiago Cintrón M. Cellulose polymorphy, crystallite size, and the segal crystallinity index. *Cellulose* 2013; 20: 583–588.
6. Moussaoui N, Rokbi M, Osmani H, et al. Extraction and characterization of fiber treatment Inula viscosa fibers as potential polymer composite reinforcement. *J Polym Environ* 2021; 29: 3779–3793.
7. Belouadah Z, Ati A, Rokbi M, et al. Optimisation Des méthodes D'extraction Et Caractérisation Mécanique De La Fibre Alfa En Vue De Son application Comme Renfort Des Matériaux composites. *J Mater Environ* 2014; 2: 51–57.
8. Mejía Osorio JC, Rodríguez Baracaldo R and Olaya Florez JJ. The influence of alkali treatment on banana fibre's mechanical properties. *Ing Invest* 2012; 32: 83–87.
9. Binoj J, Edwin Raj R, Sreenivasan V, et al. Morphological, physical, mechanical, chemical and thermal characterization of sustainable Indian areca fruit husk fibers (Areca catechu L.) as potential alternate for hazardous synthetic fibers. *J Bionic Eng* 2016; 13: 156–165.
10. De Rosa IM, Kenny JM, Puglia D, et al. Morphological, thermal and mechanical characterization of okra (Abelmoschus esculentus) fibres as potential reinforcement in

polymer composites. *Compos Sci Technol* 2010; 70: 116–122.
11. Fiore V, Scalici T and Valenza A. Characterization of a new natural fiber from Arundo donax L. as potential reinforcement of polymer composites. *Carbohydr Polym* 2014; 106: 77–83.
12. Jayaramudu J, Guduri B and Varada Rajulu A. Characterization of new natural cellulosic fabric Grewia tilifolia. *Carbohydrate Polym* 2010; 79: 847–851.
13. Ravindran D, SR SB, Sr SB, et al. Characterization of surface-modified natural cellulosic fiber extracted from the root of Ficus religiosa tree. *Int J Biol Macromol* 2020; 156: 997–1006.
14. Al-Khanbashi A, Al-Kaabi K and Hammami A. Date palm fibers as polymeric matrix reinforcement: fiber characterization. *Polym Compos* 2005; 26: 486–497.
15. An B and Kj N. Characterization of alkali treated and untreated new cellulosic fiber from Saharan aloe vera cactus leaves. *Carbohydr Polym* 2017; 174: 200–208.
16. Vijay R, James Dhilip JD, Gowtham S, et al. Characterization of natural cellulose fiber from the barks of vachellia farnesiana. *J Nat Fibers* 2022; 19: 1343–1352.
17. Manimaran P, Solai Senthil Kumar K and Prithiviraj M. Investigation of physico chemical, mechanical and thermal properties of the albizia lebbeck bark fibers. *J Nat Fibers* 2021; 18: 1151–1162.
18. Maache M, Bezazi A, Amroune S, et al. Characterization of a novel natural cellulosic fiber from Juncus effusus L. *Carbohydr Polym* 2017; 171: 163–172.
19. KılınÇ AÇ, Köktaş S, Atagür M, et al. Effect of extraction methods on the properties of althea officinalis L. fibers. *J Nat Fibers* 2018; 15: 325–336.
20. Rao KMM and Rao KM. Extraction and tensile properties of natural fibers: vakka, date and bamboo. *Compos Struct* 2007; 77: 288–295.
21. Atalie D and Gideon RK. Extraction and characterization of Ethiopian palm leaf fibers. *Research Journal of Textile and Apparel* 2018; 22: 15–25.
22. Segal L, Creely JJ, Martin A Jr, et al. An empirical method for estimating the degree of crystallinity of native cellulose using the X-ray diffractometer. *Textil Res J* 1959; 29: 786–794.
23. Vijay R, Manoharan S, Arjun S, et al. Characterization of silane-treated and untreated natural fibers from stem of Leucas aspera. *J Nat Fibers* 2020; 18: 1957–1973.
24. Raouf Khaldoune A and Rokbi M. Extraction and characterization of novel natural fiber from Centaurea melitensis plant. *J Compos Mater* 2023; 57: 913–928.
25. Meddah M, Rokbi M and Zaoui M. Extraction and characterization of novel natural lignocellulosic fibers from Malva sylvestris L. *J Compos Mater* 2023; 57: 897–912.
26. Makri H, Rokbi M, Meddah M, et al. Extraction and characterization of novel lignocellulosic fibers from Centaurea hyalolepis plant as a potential reinforcement for composite materials. *J Compos Mater* 2023; 57: 3317–3330.
27. Rokbi M, Osmani H, Imad A, et al. Effect of chemical treatment on flexure properties of natural fiber-reinforced polyester composite. *Procedia Engineering* 2011; 10: 2092–2097.
28. Reddy KO, Ashok B, Reddy KRN, et al. Extraction and characterization of novel lignocellulosic fibers from Thespesia lampas plant. *Int J Polym Anal Char* 2014; 19: 48–61.
29. Indran S, Raj RE and Sreenivasan V. Characterization of new natural cellulosic fiber from Cissus quadrangularis root. *Carbohydr Polym* 2014; 110: 423–429.
30. Subramanian K, Senthil Kumar P, Jeyapal P, et al. Characterization of ligno-cellulosic seed fibre from Wrightia Tinctoria plant for textile applications—an exploratory investigation. *Eur Polym J* 2005; 41: 853–861.
31. Kumar R, Meena A, Chopra A, et al. Keratin gene expression differences in wool follicles and sequence diversity of high glycine-tyrosine keratin-associated proteins (Kaps) in magra sheep of India. *J Nat Fibers* 2020; 17: 1257–1263.
32. Mukhtar I, Leman Z, Zainudin ES, et al. Effectiveness of alkali and sodium bicarbonate treatments on sugar palm fiber: mechanical, thermal, and chemical investigations. *J Nat Fibers* 2018; 17: 877–889.
33. Hossain MK, Dewan MW, Hosur M, et al. Effect of surface treatment and nanoclay on thermal and mechanical performances of jute fabric/biopol 'green'composites. *J Reinforc Plast Compos* 2011; 30: 1841–1856.
34. Kovačević Z, Vukušić SB and Zimniewska M. Comparison of Spanish broom (Spartium junceum L.) and flax (Linum usitatissimum) fibre. *Textil Res J* 2012; 82: 1786–1798.
35. Jabbar A, Militký J, Wiener J, et al. Tensile, surface and thermal characterization of jute fibres after novel treatments. *Indian J Fiber Textil Res* 2016; 41: 249–254.
36. Lemita N, Deghboudj S, Rokbi M, et al. Characterization and analysis of novel natural cellulosic fiber extracted from Strelitzia reginae plant. *J Compos Mater* 2022; 56: 99–114.
37. Ellefsen O, Lund EW, Tønnesen B, et al. Studies on cellulose characterization by means of X-ray methods. *Norsk Skogind* 1957; 11: 284.
38. French AD. Idealized powder diffraction patterns for cellulose polymorphs. *Cellulose* 2014; 21: 885–896.
39. Isogai A and Atalla R. Amorphous celluloses stable in aqueous media: regeneration from SO_2–amine solvent systems. *J Polym Sci Polym Chem* 1991; 29: 113–119.
40. Ju X, Bowden M, Brown EE, et al. An improved X-ray diffraction method for cellulose crystallinity measurement. *Carbohydr Polym* 2015; 123: 476–481.
41. del Cerro DR, Koso TV, Kakko T, et al. Crystallinity reduction and enhancement in the chemical reactivity of cellulose by non-dissolving pre-treatment with tetrabutylphosphonium acetate. *Cellulose* 2020; 27: 5545–5562.
42. Agarwal UP, Ralph SA, Baez C, et al. Contributions of crystalline and noncrystalline cellulose can occur in the same spectral regions: evidence based on Raman and IR and its

implication for crystallinity measurements. *Biomacromolecules* 2021; 22: 1357–1373.
43. Yao W, Weng Y and Catchmark JM. Improved cellulose X-ray diffraction analysis using fourier series modeling. *Cellulose* 2020; 27: 5563–5579.
44. French AD. Increment in evolution of cellulose crystallinity analysis. *Cellulose* 2020; 27: 5445–5448.
45. Thygesen A, Oddershede J, Lilholt H, et al. On the determination of crystallinity and cellulose content in plant fibres. *Cellulose* 2005; 12: 563–576.
46. Park S, Baker JO, Himmel ME, et al. Cellulose crystallinity index: measurement techniques and their impact on interpreting cellulase performance. *Biotechnol Biofuels* 2010; 3: 10–10.
47. Umashankaran M and Gopalakrishnan S. Effect of sodium hydroxide treatment on physico-chemical, thermal, tensile and surface morphological properties of pongamia Pinnata L. bark fiber. *J Nat Fibers* 2021; 18: 2063–2076.
48. Saravanakumar S, Kumaravel A, Nagarajan T, et al. Characterization of a novel natural cellulosic fiber from Prosopis juliflora bark. *Carbohydr Polym* 2013; 92: 1928–1933.
49. Dalmis R, Kilic GB, Seki Y, et al. Characterization of a novel natural cellulosic fiber extracted from the stem of Chrysanthemum morifolium. *Cellulose* 2020; 27: 8621–8634.
50. Arul Marcel Moshi A, Ravindran D, Sundara Bharathi SR, et al. Characterization of surface-modified natural cellulosic fiber extracted from the root of Ficus religiosa tree. *Int J Biol Macromol* 2020; 156: 997–1006.
51. Shebani A, Van Reenen A and Meincken M. The effect of wood extractives on the thermal stability of different wood species. *Thermochim Acta* 2008; 471: 43–50.
52. Siva R, Valarmathi T, Palanikumar K, et al. Study on a novel natural cellulosic fiber from Kigelia africana fruit: characterization and analysis. *Carbohydr Polym* 2020; 244: 116494.
53. Mohanta N and Acharya S. Fiber surface treatment: its effect on structural, thermal, and mechanical properties of Luffa cylindrica fiber and its composite. *J Compos Mater* 2016; 50: 3117–3131.
54. Babu B, Princewinston D, Saravanakumar S, et al. Investigation on the physicochemical and mechanical properties of novel alkali-treated Phaseolus vulgaris fibers. *J Nat Fibers* 2020; 19: 770–781.
55. Sreenivasan V, Somasundaram S, Ravindran D, et al. Microstructural, physico-chemical and mechanical characterisation of Sansevieria cylindrica fibres–an exploratory investigation. *Mater Des* 2011; 32: 453–461.
56. Pappu A, Saxena M, Thakur VK, et al. Facile extraction, processing and characterization of biorenewable sisal fibers for multifunctional applications. *J Macromol Sci, Part A* 2016; 53: 424–432.
57. Manimaran P, Senthamaraikannan P, Sanjay M, et al. Study on characterization of Furcraea foetida new natural fiber as composite reinforcement for lightweight applications. *Carbohydr Polym* 2018; 181: 650–658.
58. Noureddine M. Study of composite-based natural fibers and renewable polymers, using bacteria to ameliorate the fiber/matrix interface. *J Compos Mater* 2018; 53: 455–461.
59. Abdelhak B, Noureddine M and Hacen M. Improvement of the interfacial adhesion between fiber and matrix. *Mechanics & Mechanical Engineering* 2018; 22: 885–894.